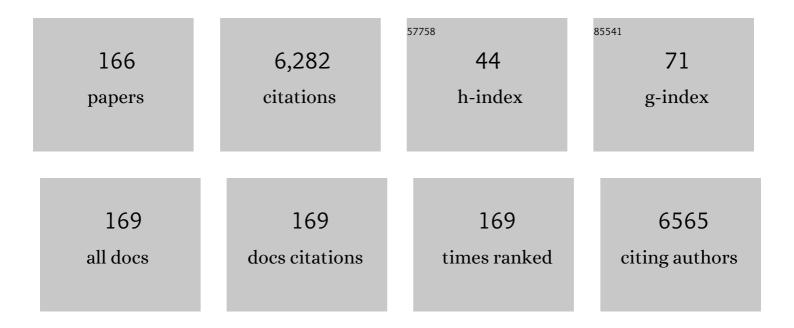
John Charles Walmsley

List of Publications by Year in descending order

Source: https://exaly.com/author-pdf/6855197/publications.pdf Version: 2024-02-01



#	Article	IF	CITATIONS
1	Effects of metal dusting relevant exposures of alloy 601 surfaces on carbon formation and oxide development. Catalysis Today, 2021, 369, 48-61.	4.4	8
2	Slow carrier relaxation in tin-based perovskite nanocrystals. Nature Photonics, 2021, 15, 696-702.	31.4	40
3	Active sites for the oxygen reduction reaction in nitrogen-doped carbon nanofibers. Catalysis Today, 2020, 357, 248-258.	4.4	28
4	Stress Corrosion Cracking in an Extruded Cu-Free Al-Zn-Mg Alloy. Metals, 2020, 10, 1194.	2.3	3
5	Copper enriched by dealloying as external cathode in intergranular corrosion of aluminium alloy AA6005. Corrosion Science, 2019, 158, 108090.	6.6	12
6	Methane Activation on Bimetallic Catalysts: Properties and Functions of Surface Niâ^'Ag Alloy. ChemCatChem, 2019, 11, 3401-3412.	3.7	16
7	Progress in Understanding Initiation of Intergranular Corrosion on AA6005 Aluminum Alloy with Low Copper Content. Journal of the Electrochemical Society, 2019, 166, C3114-C3123.	2.9	19
8	Mechanical Properties and Processing Techniques of Bulk Metal–Organic Framework Glasses. Journal of the American Chemical Society, 2019, 141, 1027-1034.	13.7	93
9	Optical response of rectangular array of elliptical plasmonic particles on glass revealed by Mueller matrix ellipsometry and finite element modeling. Journal of the Optical Society of America B: Optical Physics, 2019, 36, E78.	2.1	13
10	Decoding Atomic-Level Structures of the Interface between Pt Sub-nanocrystals and Nanostructured Carbon. Journal of Physical Chemistry C, 2018, 122, 7166-7178.	3.1	4
11	Evaluation of ORR active sites in nitrogen-doped carbon nanofibers by KOH post treatment. Catalysis Today, 2018, 301, 11-16.	4.4	36
12	Effect of composition and preparation of supported MoO3 catalysts for anisole hydrodeoxygenation. Chemical Engineering Journal, 2018, 335, 120-132.	12.7	79
13	Effects of Sulphur on a Co/Mn-based Catalyst for Fischer–Tropsch Reactions. Catalysis Letters, 2018, 148, 2980-2991.	2.6	1
14	Nitrogenâ€doped Carbon Nanofibers for the Oxygen Reduction Reaction: Importance of the Iron Growth Catalyst Phase. ChemCatChem, 2017, 9, 1663-1674.	3.7	17
15	Evaluation of Reoxidation Thresholds for γ-Al ₂ O ₃ -Supported Cobalt Catalysts under Fischer–Tropsch Synthesis Conditions. Journal of the American Chemical Society, 2017, 139, 3706-3715.	13.7	84
16	Hydrodeoxygenation of phenolics in liquid phase over supported MoO3 and carburized analogues. Biomass Conversion and Biorefinery, 2017, 7, 343-359.	4.6	18
17	TaNX coatings deposited by HPPMS on SS316L bipolar plates for polymer electrolyte membrane fuel cells: Correlation between corrosion current, contact resistance and barrier oxide film formation. International Journal of Hydrogen Energy, 2017, 42, 3259-3270.	7.1	27
18	Further insights into methane and higher hydrocarbons formation over cobalt-based catalysts with γ-Al2O3, α-Al2O3 and TiO2 as support materials. Journal of Catalysis, 2017, 352, 515-531.	6.2	28

#	Article	IF	CITATIONS
19	Novel Fe/MnK NTs nanocomposites as catalysts for direct production of lower olefins from syngas. AICHE Journal, 2017, 63, 154-161.	3.6	16
20	Charging effects and surface potential variations of Cu-based nanowires. Thin Solid Films, 2016, 601, 45-53.	1.8	14
21	Pd/CeO 2 catalysts as powder in a fixed-bed reactor and as coating in a stacked foil microreactor for the methanol synthesis. Catalysis Today, 2016, 273, 25-33.	4.4	10
22	Boosted Supercapacitive Energy with High Rate Capability of aCarbon Framework with Hierarchical Pore Structure in an Ionic Liquid. ChemSusChem, 2016, 9, 3093-3101.	6.8	33
23	Fabrication of K-promoted iron/carbon nanotubes composite catalysts for the Fischer–Tropsch synthesis of lower olefins. Journal of Energy Chemistry, 2016, 25, 311-317.	12.9	55
24	Geometrically confined favourable ion packing for high gravimetric capacitance in carbon–ionic liquid supercapacitors. Energy and Environmental Science, 2016, 9, 232-239.	30.8	109
25	Chemical stability and H2 flux degradation of cercer membranes based on lanthanum tungstate and lanthanum chromite. Journal of Membrane Science, 2016, 503, 42-47.	8.2	16
26	Nitrogen-doped carbon nanofibers on expanded graphite as oxygen reduction electrocatalysts. Carbon, 2016, 101, 191-202.	10.3	62
27	One-step electrochemical synthesis of tunable nitrogen-doped graphene. Journal of Materials Chemistry A, 2016, 4, 1233-1243.	10.3	69
28	ZnO–Carbonâ€Nanotube Composite Supported Nickel Catalysts for Selective Conversion of Cellulose into Vicinal Diols. ChemCatChem, 2015, 7, 2991-2999.	3.7	19
29	Combined X-ray and Raman Studies on the Effect of Cobalt Additives on the Decomposition of Magnesium Borohydride. Energies, 2015, 8, 9173-9190.	3.1	28
30	Titanium uptake and incorporation into silica nanostructures by the diatom Pinnularia sp. (Bacillariophyceae). Journal of Applied Phycology, 2015, 27, 777-786.	2.8	22
31	Combining HAADF STEM tomography and electron diffraction for studies of α-Al(Fe,Mn)Si dispersoids in 3xxx aluminium alloys. Philosophical Magazine, 2015, 95, 744-758.	1.6	12
32	CaO Nanoparticles Coated by ZrO ₂ Layers for Enhanced CO ₂ Capture Stability. Industrial & Engineering Chemistry Research, 2015, 54, 8929-8939.	3.7	40
33	Initiation of Metal Dusting Corrosion in Conversion of Natural Gas to Syngas Studied under Industrially Relevant Conditions. Industrial & Engineering Chemistry Research, 2014, 53, 1794-1803.	3.7	13
34	Anodic electrodeposition of Ag1â^' x Cu x O microcrystals. Journal of Solid State Electrochemistry, 2014, 18, 13-18.	2.5	0
35	Coaxial Carbon/Metal Oxide/Aligned Carbon Nanotube Arrays as Highâ€Performance Anodes for Lithium Ion Batteries. ChemSusChem, 2014, 7, 1335-1346.	6.8	29
36	X-ray absorption, X-ray diffraction and electron microscopy study of spent cobalt based catalyst in semi-commercial scale Fischer–Tropsch synthesis. Applied Catalysis A: General, 2014, 479, 59-69.	4.3	30

#	Article	IF	CITATIONS
37	Liquid metal embrittlement of aluminium by segregation of trace element gallium. Corrosion Science, 2014, 85, 167-173.	6.6	40
38	Using (S)TEM Techniques to Study Energy Related Materials at the Nanoscale. Microscopy and Microanalysis, 2014, 20, 414-415.	0.4	0
39	Surface segregation of tin by heat treatment of dilute aluminium–tin alloys. Corrosion Science, 2013, 68, 204-213.	6.6	14
40	The role of retained austenite in hydrogen embrittlement of supermartensitic stainless steel. Engineering Failure Analysis, 2013, 34, 140-149.	4.0	61
41	A combined in situ XAS-XRPD-Raman study of Fischer–Tropsch synthesis over a carbon supported Co catalyst. Catalysis Today, 2013, 205, 86-93.	4.4	48
42	Ru@Pt core–shell nanoparticles for methanol fuel cell catalyst: Control and effects of shell composition. International Journal of Hydrogen Energy, 2013, 38, 16631-16641.	7.1	64
43	Crystalline Al _{1 â^'} <i>_x</i> Ti <i>_x</i> phases in the hydrogen cycle NaAlH ₄ + 0.02TiCl ₃ system. Philosophical Magazine, 2013, 93, 1080-1094.	d _{1.6}	6
44	Effect of Trace Elements Lead and Tin on Anodic Activation of AA8006 Aluminum Sheet. Journal of the Electrochemical Society, 2013, 160, C542-C552.	2.9	11
45	Publisher's Note: ALD Applied to Conformal Coating of Nanoporous γ-Alumina: Spinel Formation and Luminescence Induced by Europium Doping [<i>J. Electrochem. Soc.</i> , 159, P45 (2012)]. Journal of the Electrochemical Society, 2012, 159, S15-S15.	2.9	0
46	Surface Segregation of Trace Element Bismuth during Heat Treatment of Aluminum. Journal of the Electrochemical Society, 2012, 159, C137-C145.	2.9	21
47	Nanoconfinement of Ni clusters towards a high sintering resistance of steam methane reforming catalysts. Catalysis Science and Technology, 2012, 2, 2476.	4.1	20
48	ALD Applied to Conformal Coating of Nanoporous Î ³ -Alumina: Spinel Formation and Luminescence Induced by Europium Doping. Journal of the Electrochemical Society, 2012, 159, P45-P49.	2.9	10
49	Oxide Coating of Alumina Nanoporous Structure Using ALD to Produce Highly Porous Spinel. Chemical Vapor Deposition, 2012, 18, 315-325.	1.3	16
50	Hydrogen Absorption Kinetics of the Transition-Metal-Chloride-Enhanced NaAlH4 System. Journal of Physical Chemistry C, 2012, 116, 14205-14217.	3.1	28
51	The location of Ti containing phases after the completion of the NaAlH4+xTiCl3 milling process. Journal of Alloys and Compounds, 2012, 513, 597-605.	5.5	18
52	Functionality of the nanoscopic crystalline Al/amorphous Al50Ti50 surface embedded composite observed in the NaAlH4+xTiCl3 system after milling. Journal of Alloys and Compounds, 2012, 514, 163-169.	5.5	14
53	Amorphous Al1â^'xTix, Al1â^'xVx, and Al1â^'xFex phases in the hydrogen cycled TiCl3, VCl3 and FeCl3 enhanced NaAlH4 systems. Journal of Alloys and Compounds, 2012, 521, 112-120.	5.5	15
54	A structural review of nanoscopic Al1â^'xTMx phase formation in the TMCIn enhanced NaAlH4 system. Journal of Alloys and Compounds, 2012, 527, 16-24.	5.5	12

#	Article	IF	CITATIONS
55	Metal Dusting Corrosion Initiation in Conversion of Natural Gas to Synthesis Gas. Energy Procedia, 2012, 26, 125-134.	1.8	5
56	Hydrogen absorption kinetics and structural features of NaAlH4 enhanced with transition-metal and Ti-based nanoparticles. International Journal of Hydrogen Energy, 2012, 37, 15175-15186.	7.1	21
57	Microstructural heterogeneity in hexagonal close-packed pure Ti processed by high-pressure torsion. Journal of Materials Science, 2012, 47, 4838-4844.	3.7	18
58	Initial Studies of 6082 Aluminium Thin Films. , 2012, , 245-250.		0
59	ALD Applied to Conformal Coating of Nanoporous Î ³ -Alumina: Spinel Formation and Luminescence Induced by Europium Doping. ECS Transactions, 2011, 41, 123-130.	0.5	8
60	Formation of ZnO Nanosheets Grown by Catalyst-Assisted Pulsed Laser Deposition. Crystal Growth and Design, 2011, 11, 5298-5304.	3.0	19
61	TEM characterization of pure and transition metal enhanced NaAlH4. Journal of Alloys and Compounds, 2011, 509, 281-289.	5.5	30
62	H-initiated extended defects from plasma treatment: Comparison between c-Si and mc-Si. Journal of Physics: Conference Series, 2011, 281, 012029.	0.4	2
63	Study of intergrown L and Q′ precipitates in Al–Mg–Si–Cu alloys. Scripta Materialia, 2011, 64, 817-820.	5.2	84
64	Quantitative analysis of grain refinement in titanium during equal channel angular pressing. Scripta Materialia, 2011, 64, 904-907.	5.2	91
65	In-Situ Reduction of Promoted Cobalt Oxide Supported on Alumina by Environmental Transmission Electron Microscopy. Catalysis Letters, 2011, 141, 754-761.	2.6	49
66	Effect of water on the space-time yield of different supported cobalt catalysts during Fischer–Tropsch synthesis. Applied Catalysis A: General, 2011, 393, 109-121.	4.3	62
67	Vapor–solid–solid Si nano-whiskers growth using pure hydrogen as the source gas. Thin Solid Films, 2011, 519, 4613-4616.	1.8	2
68	Surface Characterization of Heat Treated AlPbCu Model Alloys. Journal of the Electrochemical Society, 2011, 158, C178.	2.9	5
69	Deformation Structures of Pure Titanium during Shear Deformation. Metallurgical and Materials Transactions A: Physical Metallurgy and Materials Science, 2010, 41, 787-794.	2.2	50
70	Faceted interfacial structure of {101Â ⁻ 1} twins in Ti formed during equal channel angular pressing. Scripta Materialia, 2010, 62, 443-446.	5.2	68
71	The effects of ball milling intensity on morphology of multiwall carbon nanotubes. Scripta Materialia, 2010, 63, 637-640.	5.2	45
72	On the selectivity of cobalt-based Fischer–Tropsch catalysts: Evidence for a common precursor for methane and long-chain hydrocarbons. Journal of Catalysis, 2010, 274, 84-98.	6.2	92

#	Article	IF	CITATIONS
73	Inactive aluminate spinels as precursors for design of CPO and reforming catalysts. Applied Catalysis A: General, 2010, 383, 119-127.	4.3	35
74	Microstructure evolution of commercial pure titanium during equal channel angular pressing. Materials Science & Engineering A: Structural Materials: Properties, Microstructure and Processing, 2010, 527, 789-796.	5.6	80
75	Ethene production by oxidative dehydrogenation of ethane at short contact times over Pt-Sn coated monoliths. Applied Catalysis A: General, 2010, 378, 1-10.	4.3	28
76	Surface characterization of Pd/Ag23wt% membranes after different thermal treatments. Applied Surface Science, 2010, 256, 6121-6132.	6.1	32
77	Characterization of thin and ultrathin transparent conducting oxide (TCO) films and TCOâ€Si interfaces with XPS, TEM and <i>ab initio</i> modeling. Surface and Interface Analysis, 2010, 42, 874-877.	1.8	7
78	The influence of composition and natural aging on clustering during preaging in Al–Mg–Si alloys. Journal of Applied Physics, 2010, 108, .	2.5	120
79	Importance of Oxygen-Free Edge and Defect Sites for the Immobilization of Colloidal Pt Oxide Particles with Implications for the Preparation of CNF-Supported Catalysts. Journal of Physical Chemistry C, 2010, 114, 1752-1762.	3.1	53
80	The evolution and oxidation of carbides in an Alloy 601 exposed to long term high temperature corrosion conditions. Corrosion Science, 2010, 52, 4001-4010.	6.6	9
81	Multilayer Corrosion of Aluminum Activated by Lead. Journal of the Electrochemical Society, 2010, 157, C313.	2.9	26
82	Effect of Excess Silicon and Small Copper Content on Intergranular Corrosion of 6000-Series Aluminum Alloys. Journal of the Electrochemical Society, 2010, 157, C61.	2.9	89
83	Si substrates texturing and vapor-solid-solid Si nanowhiskers growth using pure hydrogen as source gas. Journal of Applied Physics, 2009, 105, 043507.	2.5	1
84	Transmission electron microscopy study of hydrogen defect formation at extended defects in hydrogen plasma treated multicrystalline silicon. Journal of Applied Physics, 2009, 105, 033506.	2.5	18
85	Characterization of ZnO Nanostructures Grown by Pulsed Laser Deposition. Materials Research Society Symposia Proceedings, 2009, 1174, 115.	0.1	Ο
86	On nanoscale Al precipitates forming in eutectic Si particles in Al–Si–Mg cast alloys. Scripta Materialia, 2009, 61, 500-503.	5.2	12
87	The nature of active chromium species in Cr-catalysts for dehydrogenation of propane: New insights by a comprehensive spectroscopic study. Journal of Catalysis, 2009, 261, 116-128.	6.2	150
88	Microstructural studies of self-supported (1.5–10 μm) Pd/23Âwt%Ag hydrogen separation membranes subjected to different heat treatments. Journal of Materials Science, 2009, 44, 4429-4442.	3.7	23
89	Co–Ni Catalysts Derived from Hydrotalcite-Like Materials for Hydrogen Production by Ethanol Steam Reforming. Topics in Catalysis, 2009, 52, 206-217.	2.8	133
90	Hydrogen Oxidation Catalyzed by Pt Supported on Carbon Nanofibers with Different Graphite Sheet Orientations. Topics in Catalysis, 2009, 52, 664-674.	2.8	10

#	Article	IF	CITATIONS
91	Observations of nanoscopic, face centered cubic Ti and TiH x. Applied Physics A: Materials Science and Processing, 2009, 94, 787-793.	2.3	12
92	Study of defects and impurities in multicrystalline silicon grown from metallurgical silicon feedstock. Materials Science and Engineering B: Solid-State Materials for Advanced Technology, 2009, 159-160, 274-277.	3.5	23
93	Thin Pd–23%Ag/stainless steel composite membranes: Long-term stability, life-time estimation and post-process characterisation. Journal of Membrane Science, 2009, 326, 572-581.	8.2	96
94	Effects of thermal activation on hydrogen permeation properties of thin, self-supported Pd/Ag membranes. Separation and Purification Technology, 2009, 68, 403-410.	7.9	46
95	Dehydrogenation of propane over Pt-SBA-15 and Pt-Sn-SBA-15: Effect of Sn on the dispersion of Pt and catalytic behavior. Catalysis Today, 2009, 142, 17-23.	4.4	128
96	Composition of β″ precipitates in Al–Mg–Si alloys by atom probe tomography and first principles calculations. Journal of Applied Physics, 2009, 106, .	2.5	185
97	Microstructural characterization of self-supported 1.6μm Pd/Ag membranes. Journal of Membrane Science, 2008, 310, 337-348.	8.2	35
98	Preparation and characterization of nanocrystalline, high-surface area CuCeZr mixed oxide catalysts from homogeneous co-precipitation. Chemical Engineering Journal, 2008, 137, 686-702.	12.7	26
99	Electron Microscopy Study of γ-Al2O3 Supported Cobalt Fischer–Tropsch Synthesis Catalysts. Catalysis Letters, 2008, 126, 224-230.	2.6	33
100	A Model for High-Temperature Pitting Corrosion in Nickel-Based Alloys Involving Internal Precipitation of Carbides, Oxides, and Graphite. Metallurgical and Materials Transactions A: Physical Metallurgy and Materials Science, 2008, 39, 1258-1276.	2.2	23
101	Hydrodesulfurization of thiophene on carbon nanofiber supported Co/Ni/Mo catalysts. Applied Catalysis B: Environmental, 2008, 84, 482-489.	20.2	49
102	Structural properties of the nanoscopic Al85Ti15 solid solution observed in the hydrogen-cycled NaAlH4+ 0.1TiCl3 system. Acta Materialia, 2008, 56, 4691-4701.	7.9	30
103	Performance and SEM characterization of Rh impregnated microchannel reactors in the catalytic partial oxidation of methane and propane. Chemical Engineering Journal, 2008, 144, 489-501.	12.7	28
104	The effect of platinum in Cu-Ce-Zr and Cu-Zn-Al mixed oxide catalysts for water–gas shift. Applied Catalysis A: General, 2008, 349, 46-54.	4.3	16
105	Fischer–Tropsch synthesis: Cobalt particle size and support effects on intrinsic activity and product distribution. Journal of Catalysis, 2008, 259, 161-164.	6.2	297
106	Dehydrogenation of propane over Pt-SBA-15: Effect of Pt particle size. Catalysis Communications, 2008, 9, 747-750.	3.3	113
107	The Structure and Impurities of Hard DC Anodic Layers on AA6060 Aluminium Alloy. Journal of Adhesion, 2008, 84, 543-561.	3.0	12
108	Characterization of nanostructured GaSb: comparison between large-area optical and local direct microscopic techniques. Applied Optics, 2008, 47, 5130.	2.1	20

#	Article	IF	CITATIONS
109	Effect of Magnesium on Segregation of Trace Element Lead and Anodic Activation in Aluminum Alloys. Journal of the Electrochemical Society, 2008, 155, C1.	2.9	8
110	EBIC, EBSD and TEM study of grain boundaries in multicrystalline silicon cast from metallurgical feedstock. Conference Record of the IEEE Photovoltaic Specialists Conference, 2008, , .	0.0	5
111	Toward Three-Dimensional Nanoengineering of Heterogeneous Catalysts. Journal of the American Chemical Society, 2008, 130, 5716-5719.	13.7	63
112	Intergranular Corrosion of Copper-Containing AA6xxx AlMgSi Aluminum Alloys. Journal of the Electrochemical Society, 2008, 155, C550.	2.9	102
113	Silicon Whisker Growth Using Hot Filament Reactor with Hydrogen as Source Gas. Japanese Journal of Applied Physics, 2008, 47, 4807-4809.	1.5	6
114	Transmission electron microscopy characterization of NaAlH ₄ . Journal of Physics: Conference Series, 2008, 126, 012015.	0.4	2
115	Nature of Segregated Lead on Electrochemically Active AlPb Model Alloy. Journal of the Electrochemical Society, 2007, 154, C28.	2.9	21
116	A Comparative Analysis of Structural Defect Formation in Si ⁺ Implanted and then Plasma Hydrogenated and in H ⁺ Implanted Crystalline Silicon. Solid State Phenomena, 2007, 131-133, 309-314.	0.3	1
117	The Temperature Evolution of the Hydrogen Plasma Induced Structural Defects in Crystalline Silicon. Solid State Phenomena, 2007, 131-133, 315-320.	0.3	5
118	The effect of Cu on precipitation in Al–Mg–Si alloys. Philosophical Magazine, 2007, 87, 3385-3413.	1.6	238
119	Comparative study of the β″-phase in a 6xxx Al alloy by 3DAP and HRTEM. Surface and Interface Analysis, 2007, 39, 189-194.	1.8	24
120	Wet air oxidation in a catalytic membrane reactor: Model and industrial wastewaters in single tubes and multichannel contactors. Applied Catalysis B: Environmental, 2007, 69, 196-206.	20.2	22
121	Nanocrystalline Cu-Ce-Zr mixed oxide catalysts for water-gas shift: Carbon nanofibers as dispersing agent for the mixed oxide particles. Applied Catalysis B: Environmental, 2007, 71, 7-15.	20.2	29
122	Ni catalysts for sorption enhanced steam methane reforming. Topics in Catalysis, 2007, 45, 3-8.	2.8	32
123	Platinum incorporated into the SBA-15 mesostructure via deposition-precipitation method: Pt nanoparticle size estimation and catalytic testing. Topics in Catalysis, 2007, 45, 93-99.	2.8	31
124	Z-contrast imaging of the arrangement of Cu in precipitates in 6XXX-series aluminium alloys. Philosophical Magazine Letters, 2006, 86, 589-597.	1.2	21
125	Effect of artificial aging on intergranular corrosion of extruded AlMgSi alloy with small Cu content. Corrosion Science, 2006, 48, 1528-1543.	6.6	176
126	Characterisation of early precipitation stages in 6xxx series aluminium alloys. Journal of Physics: Conference Series, 2006, 26, 99-102.	0.4	0

#	Article	IF	CITATIONS
127	Studies of self-supported 1.6î¼m Pd/23wt.% Ag membranes during and after hydrogen production in a catalytic membrane reactor. Catalysis Today, 2006, 118, 63-72.	4.4	48
128	Evolution of hydrogen induced defects during annealing of plasma treated Czochralski silicon. Nuclear Instruments & Methods in Physics Research B, 2006, 253, 176-181.	1.4	12
129	Surface Segregation of Indium by Heat Treatment of Aluminium. Materials Science Forum, 2006, 519-521, 673-678.	0.3	10
130	Significance of Low Copper Content on Grain Boundary Nanostructure and Intergranular Corrosion of AlMgSi(Cu) Model Alloys. Materials Science Forum, 2006, 519-521, 667-672.	0.3	13
131	Effect of Heat Treatment on Grain Boundary Nanostructure and Corrosion of Low Copper AlMgSi Alloy. ECS Transactions, 2006, 3, 167-172.	0.5	6
132	Platinum nanoparticles encapsulated in mesoporous silica: Preparation, characterisation and catalytic activity in toluene hydrogenation. Microporous and Mesoporous Materials, 2005, 86, 198-206.	4.4	62
133	Catalytic membrane structure influence on the pressure effects in an interfacial contactor catalytic membrane reactor applied to wet air oxidation. Catalysis Today, 2005, 104, 329-335.	4.4	27
134	Characterization of alumina-, silica-, and titania-supported cobalt Fischer–Tropsch catalysts. Journal of Catalysis, 2005, 236, 139-152.	6.2	182
135	Electron-microscopy studies of NaAlH4 with TiF3 additive: hydrogen-cycling effects. Applied Physics A: Materials Science and Processing, 2005, 80, 709-715.	2.3	53
136	Small-scale hydrogen production from propane. Catalysis Today, 2005, 100, 457-462.	4.4	53
137	Synthesis and Characterization of Gold Nanoparticleâ€Functionalized Ordered Mesoporous Materials. Journal of Dispersion Science and Technology, 2005, 26, 729-744.	2.4	13
138	Transmission Electron Microscopy Studies of 5-cycled Na Alanate with Ti Based Additive. Materials Research Society Symposia Proceedings, 2005, 884, 1.	0.1	0
139	Analytical Electron Microscopy Studies of Lithium Aluminum Hydrides with Ti- and V-Based Additives. Journal of Physical Chemistry B, 2005, 109, 4350-4356.	2.6	21
140	Electron microscopy studies of lithium aluminium hydrides. Journal of Alloys and Compounds, 2005, 395, 307-312.	5.5	23
141	Formation and characterisation of a chromate conversion coating on AA6060 aluminium. Corrosion Science, 2005, 47, 1604-1624.	6.6	92
142	Effects of Silica Nano-Particle Coatings on High-Temperature Oxidation of AISI 321. Materials Science Forum, 2004, 461-464, 281-288.	0.3	0
143	The effect of pre-bond moisture on epoxy-bonded sulphuric acid anodised aluminium. International Journal of Adhesion and Adhesives, 2004, 24, 183-191.	2.9	16
144	Performance of catalytic membrane reactor in multiphase reactions. Chemical Engineering Science, 2004, 59, 5363-5372.	3.8	21

#	Article	IF	CITATIONS
145	Microscale investigations of the metal-dusting corrosion mechanism on mild steel. Metallurgical and Materials Transactions A: Physical Metallurgy and Materials Science, 2003, 34, 345-354.	2.2	6
146	Anodising as pre-treatment for structural bonding. International Journal of Adhesion and Adhesives, 2003, 23, 401-412.	2.9	83
147	Electron microscopy studies of a TbNiAl compound processed by the HDDR route. Journal of Alloys and Compounds, 2003, 356-357, 658-663.	5.5	2
148	Formation of a zirconium-titanium based conversion layer on AA 6060 aluminium. Surface and Coatings Technology, 2002, 153, 72-78.	4.8	126
149	Microstructure and the influence of spontaneous strain in LaCoO3, La0.8Sr0.2CoO3 and La0.8Ca0.2CoO3. Journal of Materials Science, 2000, 35, 4251-4260.	3.7	22
150	Mechanisms of inclusion formation in low alloy steels deoxidised with titanium. Materials Science and Technology, 2000, 16, 55-64.	1.6	45
151	Importance of Molybdenum on Irradiation-Assisted Stress Corrosion Cracking in Austenitic Stainless Steels. Corrosion, 1998, 54, 48-60.	1.1	25
152	Defect annealing and the formation of Li-rich clusters in Al-Li alloys. Journal of Physics Condensed Matter, 1995, 7, 4573-4581.	1.8	3
153	Observations of changing fine structure in nanoscale EELS analysis of grain boundaries in stainless steels. Journal of Microscopy, 1995, 180, 313-325.	1.8	4
154	Atomic number contrast imaging and microanalysis of copper precipitates in irradiated ferritic pressure vessel steels. Philosophical Magazine Letters, 1993, 67, 131-136.	1.2	1
155	Large ã€^110〉-segmented helical dislocations in natural diamond. Philosophical Magazine Letters, 1992, 65, 159-165.	1.2	3
156	Study of a platelet-free infilling of a crack in natural diamond: evidence for a late growth event. Journal of Crystal Growth, 1992, 116, 225-234.	1.5	4
157	The relationship between platelet size and the frequency of the B' infrared absorption peak in type la diamond. The Philosophical Magazine: Physics of Condensed Matter B, Statistical Mechanics, Electronic, Optical and Magnetic Properties, 1990, 62, 115-128.	0.6	27
158	Characteristics of diamond regrowth in a synthetic diamond compact. Journal of Materials Science, 1988, 23, 1829-1834.	3.7	22
159	The microstructure of ultrahard material compacts studied by transmission electron microscopy. Materials Science & Engineering A: Structural Materials: Properties, Microstructure and Processing, 1988, 105-106, 549-553.	5.6	9
160	Newly observed microscopic planar defects on {111} in natural diamond. Philosophical Magazine Letters, 1987, 55, 209-213.	1.2	16
161	A transmission electron microscope study of a cubic boron nitride-based compact material with AIN and AIB2 binder phases. Journal of Materials Science, 1987, 22, 4093-4102.	3.7	17
162	Transmission electron microscopic observations of deformation and microtwinning in a synthetic diamond compact. Journal of Materials Science Letters, 1983, 2, 785-788.	0.5	27

#	Article	IF	CITATIONS
163	Apatite inclusions in natural diamond coat. Physics and Chemistry of Minerals, 1983, 9, 6-8.	0.8	45
164	Wavefront dislocations in the Aharonov-Bohm effect and its water wave analogue. European Journal of Physics, 1980, 1, 154-162.	0.6	196
165	Investigation of Grain Boundaries in an Al-Mg-Si-Cu Alloy. Materials Science Forum, 0, 794-796, 951-956.	0.3	11
166	Nanostructural Analysis of Coâ€Re/γâ€Al2O3 Fischerâ€Tropsch Catalyst by TEM and XRD. ChemCatChem, 0, , .	3.7	0